The Marine Optical BuoY (MOBY) Radiometric Calibration and Uncertainty Budget for Ocean Color Satellite Sensor Vicarious Calibration

Steven W. Brown[a], Stephanie J. Flora[b],Michael E. Feinholz[b], Mark A. Yarbrough[b], Terrence Houlihan[b], Darryl Peters[b], Yong Sung Kim[c], James L. Mueller[d], B. Carol Johnson [a], and Dennis K. Clark[e]

[a]National Institute of Standards and Technology, Gaithersburg, MD USA 20899;
[b]Moss Landing Marine Laboratories, Moss Landing, CA USA 95039;
[c]Perot Systems Corporation, 4500 Forbes Blvd #200, Lanham, MD USA 20706;
[d]CHORS, San Diego State University, San Diego, CA USA 92120;
[e]Marine Optical Consulting, Arnold, MD USA 49406

ABSTRACT

For the past decade, the Marine Optical Buoy (MOBY), an autonomous radiometric buoy stationed in the waters off Lanai, Hawaii, has been the primary in-water oceanic observatory for the vicarious calibration of U. S. satellite ocean color sensors, including the Sea-viewing Wide Field-of-view Sensor (SeaWiFS) and the Moderate Resolution Imaging Spectrometer (MODIS) instruments on the National Aeronautics and Space Administration's (NASA's) Terra and Aqua satellites. The MOBY vicarious calibration of these sensors supports international efforts to develop a global, multi-year time series of consistently calibrated ocean color data products. A critical component of the MOBY program is establishing radiometric traceability to the International System of Units (SI) through standards provided by the U. S. National Institute of Standards and Technology (NIST). A detailed uncertainty budget is a core component of traceable metrology. We present the MOBY uncertainty budget for up-welling radiance and discuss approaches in new instrumentation to reduce the uncertainties in *in situ* water-leaving radiance measurements.

Keywords: calibration, Marine Optical Buoy, ocean color, satellite sensor, uncertainty

1. INTRODUCTION

The optical properties of seawater reflect its composition. Under natural illumination from sunlight, radiometric measurements of the light leaving the ocean contain information about the nature and concentration of near-surface dissolved and suspended materials. Quantitative measurements of global ocean radiance distributions by satellite sensors can yield a variety of relevant information regarding the state of the world's oceans. For example, time series of phytoplankton chlorophyll-*a* distributions from NASA's SeaWiFS and MODIS Terra and Aqua satellite sensors are used to calculate the mean and variability of basin- to global-scale primary production; to quantify the impacts of the El Nino Southern Oscillation (ENSO) and other climate signals on ocean phytoplankton biomass and productivity; to determine seasonal cycles of phytoplankton biomass on regional to global scales; to provide new quantitative insights into the relations between biological and circulation/mixing processes on daily to seasonal timescales; and to improve calculations of upper ocean heat budgets owing to phytoplankton absorption of solar irradiance [1].

Pre-launch laboratory-based radiometric calibration uncertainties of SeaWiFS and MODIS were approximately 5 %. Typically, in clear water, the contribution of the water leaving reflectance propagated to the top of the atmosphere is approximately 10 % in the blue (around 440 nm), 5% in the green (around 550 nm) and negligible in the near infrared (wavelengths greater than 750 nm) [2]. To achieve a radiometric uncertainty of 5 % in water-leaving radiance, the uncertainty dictated by uncertainty requirements in the data products, the at-sensor radiometric uncertainty requirement is 0.5 %, k=1. This level of uncertainty cannot be achieved in the laboratory and transferred on-orbit through the launch. Consequently, ocean color satellite sensor calibration is achieved vicariously, using *in situ* water-leaving radiance data obtained under well-defined conditions [2]. MOBY has provided accurate, hyperspectral water-leaving radiance data for

ocean color satellite sensors for the past decade using in-water radiometric measurements at its mooring site located in the lee of Lanai, Hawaii 20 km from the coast in 1200 m of water [3, 4].

Many of the temporal trends observed in remote sensing data products, including ocean color data products, are subtle, slowly changing, and embedded in large natural variations. Detecting small changes in long-term trends in the environment data record requires that data sets from different sensors be merged [5]. In addition, U. S. earth-observing satellite programs are transitioning to the Integrated Earth Observation System (IEOS) within the Global Earth Observation System of Systems (GEOSS). GEOSS will provide comprehensive, coordinated Earth observations from thousands of instruments worldwide, incorporating data sets from more than 70 countries and 40 international organizations. Proper interpretation of these international, multi-sensor merged data sets requires traceable metrology. Traceability in this context has a specific meaning, defined in the *International Vocabulary of Basic and General Terms in Metrology* [6] as the "property of the result of a measurement or the value of a standard whereby it can be related to stated references, usually national or international standards, through an unbroken chain of comparisons all having stated uncertainties." Within this framework, evaluation and documentation of uncertainty in measurements is an integral part in establishing traceability.

To establish direct traceability to primary national radiometric standards, the U. S. National Oceanic and Atmospheric Administration (NOAA), with support from NASA, developed a radiometric calibration validation program with NIST, the national metrology laboratory of the United States, concurrent with the development of the MOBY instrument. Through this program, rigorous measurement protocols were instituted ensuring direct traceability to primary national radiometric standards. In addition, NIST staff worked directly with the MOBY team to establish the radiometric uncertainty budget [7] and to reduce primary radiometric uncertainty components where feasible. In this work, we present an overview of the efforts undertaken by the MOBY program to ensure measurement traceability to the International System of Units (SI). Specifically, we present the uncertainty budget for up-welling radiance measured by the top MOBY arm and discuss several of the prominent components. Using the uncertainty budget for guidance, potential approaches for reducing the uncertainty budget in a new system are presented.

2. THE MARINE OPTICAL BUOY (MOBY)

MOBY is a spar buoy tethered to a slack-line moored buoy to prevent drifting. MOBY is oriented vertically in the water column, extending from the ocean surface to a depth of 12 m at the buoy's base (Fig. 1). The surface float for the buoy is 1.7 m in diameter with four 40 W solar panels mounted to the central support column. The float houses the controlling computers, data storage, electronics, cellular modem, global positioning system receiver, and computer battery. Radiometric data are collected using the Marine Optical System (MOS), located in the instrument bay at the base of the buoy, along with four 200 A/h marine batteries. The MOS system contains two spectrographs, one to measure light in the near ultraviolet and visible from 340 nm to 640 nm (the blue spectrograph), and one to measure light in the red and near infrared from 550 nm to 955 nm (the red spectrograph). The schematic diagram of MOS is shown in Fig. 2.

MOBY measures the up-welling radiance (L_u's) and down-welling irradiance (E_d's) within the ocean using remote collectors positioned on three arms oriented perpendicular to the buoy's central column. The arms can be positioned along the central column at varying depths, but are typically positioned at depths of 1 m, 5 m, and 9 m. In addition, the incident solar irradiance (E_s) is measured 2.5 m above the surface float and the up-welling radiance is measured through a window in the bottom of the instrument bay. The remote collectors are connected to 1 mm core diameter, ultraviolet-transmitting, silica-silica fiber-optic cables that are terminated at a fiber-optic rotary selector (multiplexer). This optical multiplexer is mounted on one of the entrance windows of the MOS spectrograph, and light is transmitted into the MOS optical train, through the spectrographs, and then onto the thermoelectrically cooled CCD detectors. The optical and ancillary data from MOS are relayed to the surface computer and stored on disk. The data are subsequently downloaded via a cellular telephone link. A typical MOBY data set is shown in Fig. 3. Data sets are acquired daily for the nominal satellite equatorial crossing times for SeaWiFS, MODIS Terra and MODIS Aqua overpasses. Additionally, internal reference lamps and LEDs are logged daily as a monitor of the system stability.

There are two active buoys; one is being refurbished and readied for deployment while the second buoy is deployed; typical deployments last 3 months. A separate MOS system is used in each of the two MOBY buoys. MOS204 is used in even buoy deployments while MOS205 is used in odd buoy deployments.

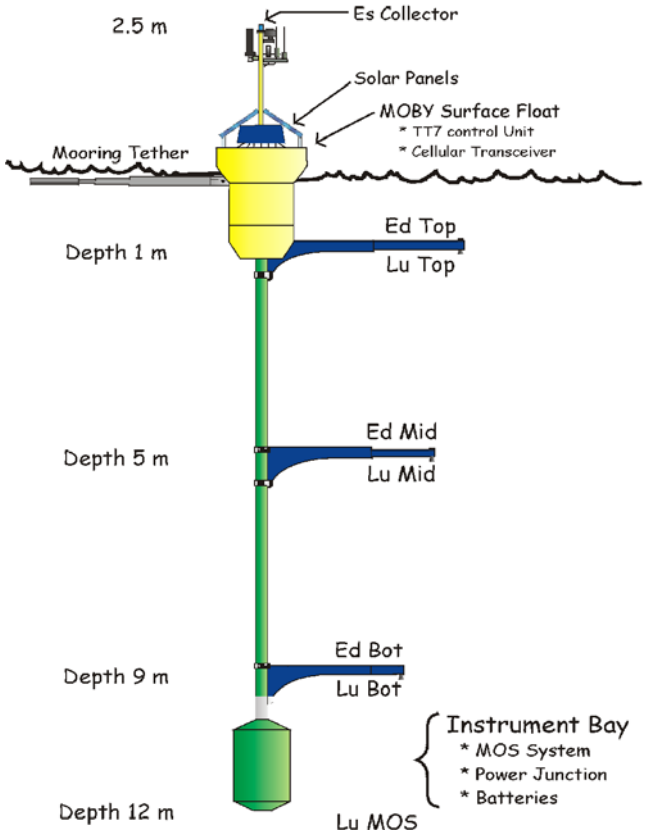

Fig. 1. Schematic diagram of MOBY.

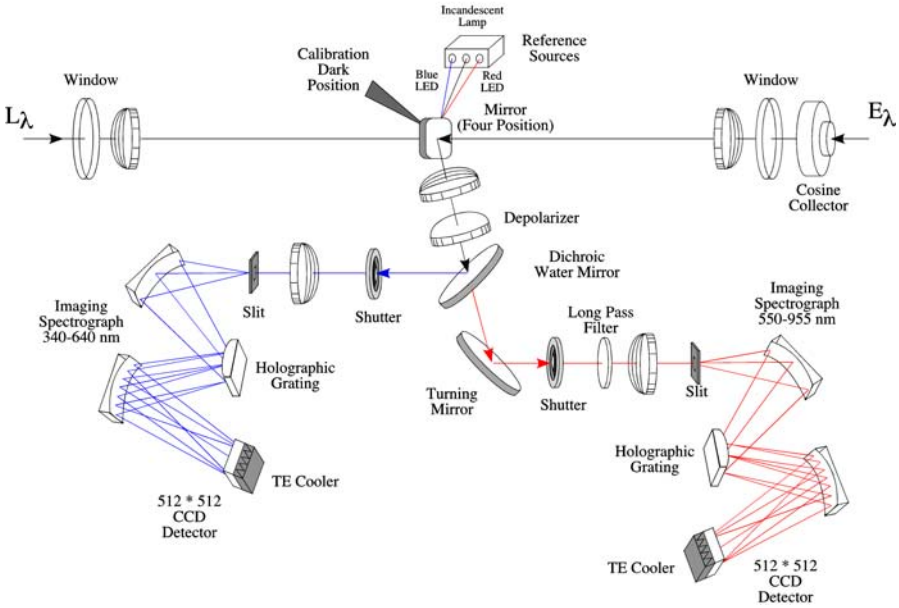

Fig. 2. Schematic diagram of the Marine Optical System.

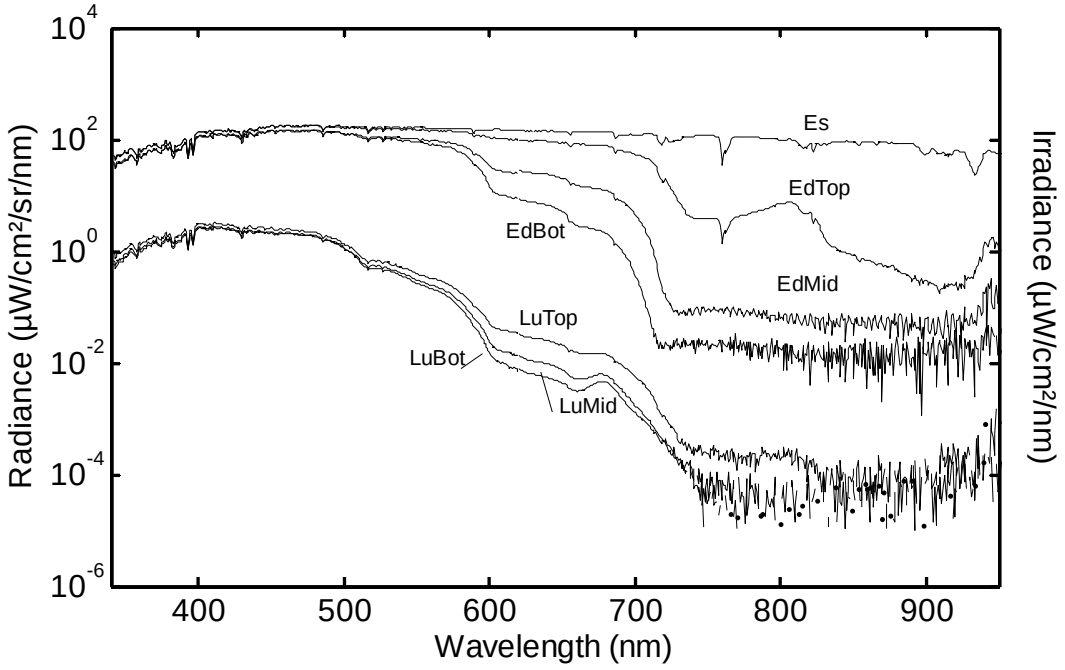

Fig. 3. A typical MOBY data set.

3. THE MEASUREMENT EQUATION [7]

MOBY makes measurements at three depths near the ocean surface. The shallowest measurements (at 1 m) are propagated upward to just below the ocean surface by calculating the up-welling spectral radiance attenuation coefficient $K_L(\lambda)$ using

$$K_L(\lambda) = \frac{1}{z_2 - z_1} \ln\left[\frac{L_u(z_1,\lambda)}{E_s^{t1}(\lambda)} \frac{E_s^{t2}(\lambda)}{L_u(z_2,\lambda)}\right] \tag{1}$$

where λ is the wavelength and z_1 and z_2 are the two depths at which measurements are made ($z_1<z_2$). The solar irradiances E_s^{t1} and E_s^{t2} are the averages of the E_s measurements before and after the in-water L_u measurements to remove the effects of solar irradiance changes from those measurements. The convention for this calculation is that the depth at the surface is zero and that the values of z increase with depth. Then the radiance change between depth z_1 and the surface is calculated using

$$L_u(0,\lambda) = L_u(z_1,\lambda)\exp[K_L(\lambda)z_1]. \tag{2}$$

The propagation of the upwelling radiance through the ocean surface, that is, the calculation of the water-leaving radiance, is accomplished using

$$L_w(0,\lambda) = \frac{T_F}{n^2} L_u(0,\lambda), \tag{3}$$

where $L_w(0,\lambda)$ is the water-leaving radiance, n is the index of refraction of water, and T_F is the Fresnel transmittance of the air-sea interface [8]. The time-averaged value of T_F for the ocean surface, as a function of wind speed at the surface, has been given by Austin [9]. These calculations assume the transmission of light along a vertical path through the ocean and the ocean surface, providing the spectral radiance for a nadir-viewing instrument immediately above the ocean surface. In practice, these calculations are complicated by the angular dependence of the upwelling radiance [10, 11], the angular dependence of the water-leaving radiance, and the Fresnel transmittance. For MOBY measurements, the

propagation of light to the surface is made from the topmost arm of the buoy (z_1=1 m). However, there are periods when the topmost arm is either broken or missing. For these periods, the center arm (z_1=5 m) is used in its place.

Finally, for comparisons with satellite-borne ocean color instruments, the high-resolution water-leaving radiance spectra from MOBY are convolved with the spectral responses of the satellite bands to form band-averaged spectral radiances. Figure 4 shows a 9 year time series of water-leaving radiance for MODIS bands, for the 22 H (GMT) satellite overpass.

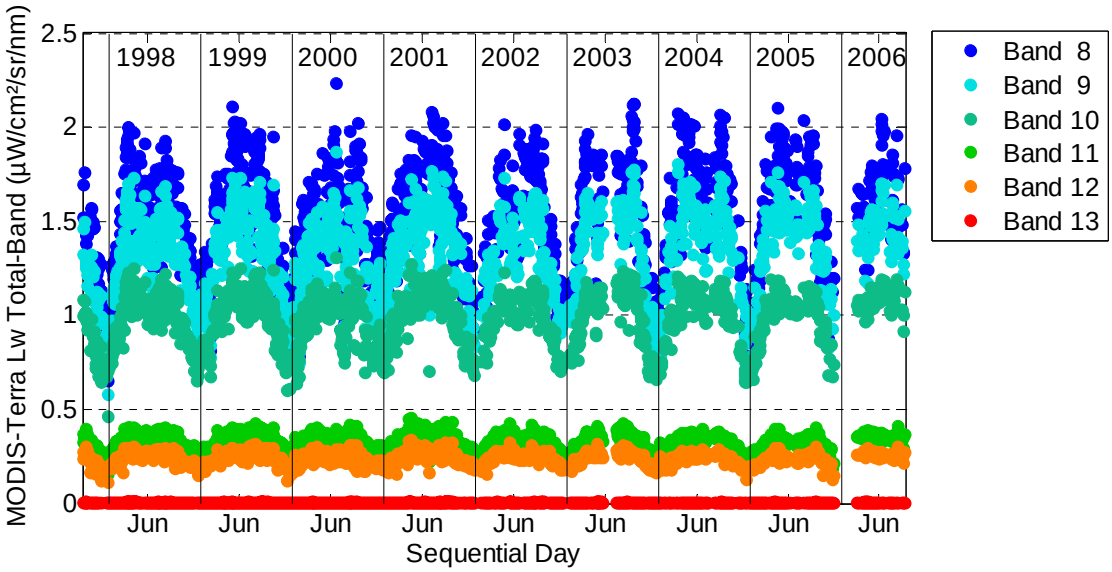

Fig. 4. MOBY time series of water-leaving radiance for MODIS ocean color bands 8 through 13.

4. THE UNCERTAINTY BUDGET

For simplicity, the uncertainty budget for the up-welling radiance measured by the top MOBY arm is considered rather than the uncertainty in the water-leaving radiance. The uncertainty budget for MODIS bands 8 through 13 will be presented. The uncertainty budget can be grouped into 4 categories: the uncertainty in the radiometric calibration sources, the uncertainty in the transfer of the radiometric scale(s) to MOBY, the radiometric stability of MOBY during a deployment, and environmental uncertainties during a measurement. The uncertainty budget, with primary components listed, is given in Table 1. While it is beyond the scope of this paper to go into the details of each element in the uncertainty budget, the prominent components will be discussed. The uncertainty in the spectral radiance of the calibration sources comes from NIST-calibrated sources. Secondary laboratories originally calibrated the sources, but the uncertainties in those calibrations – 3 % to 5 % – were too large, given a target combined standard uncertainty in the in-water measurements of similar magnitude. All sources are re-calibrated at NIST at 50 hour lamp burn intervals. The uncertainty in the stability of the calibration sources is based on repeated NIST calibrations.

In the transfer to MOBY, two uncertainty components, stray light and temperature, represent estimates of the residual uncertainties after correction. The stray light correction required several years of work and the development of a new algorithm to correct spectrograph response for stray light in the system [12, 13]. Uncorrected, stray light in the MOBY spectrographs causes a systematic error in the up-welling radiance measurement as large as 7.8 % for the 412 nm channel [12]. The temperature dependence of the MOS system was measured by building a custom variable temperature water bath large enough to hold the MOS radiometer. The radiometric response of MOS was then correlated with the temperature readings of several sensors located in different regions within the MOS instrument itself. A spectrally invariant, 0.5 %/^{o}C temperature dependence to the MOS responsivity was measured. Uncorrected, measurement errors up to several per cent due to the temperature dependence of the responsivity were commonly observed.

For *in situ* measurements of the up-welling radiance, there are uncertainty components associated with the radiometric stability of the system during a deployment and uncertainties associated with the measurement itself due to varying

Table 1. Uncertainty in $L_u(Top)$

Uncertainty Component [%]	8	9	10	11	12	13
	411.8 nm	442.1 nm	486.9 nm	529.7 nm	546.8 nm	665.6 nm
Responsivity						
Radiometric Calibration Source						
Spectral radiance	0.65	0.60	0.53	0.47	0.45	0.35
Stability	0.41	0.46	0.51	0.53	0.53	0.48
Transfer to MOBY						
Interpolation to MOBY wavelengths	0.2	0.15	0.03	0.03	0.03	0.03
Reproducibility	0.37	0.39	0.42	0.44	0.42	0.3
Wavelength accuracy	0.29	0.08	0.04	0.03	0.01	0.04
Stray light	0.75	0.3	0.1	0.15	0.3	0.3
Temperature	0.25	0.25	0.25	0.25	0.25	0.25
Measurements of L_u						
MOBY stability during deployment						
System response	1.59	1.3	1.19	1.11	1.08	0.92
In-water internal calibration	0.43	0.42	0.44	0.46	0.51	0.55
Wavelength stability	0.132	0.138	1.122	0.816	1.368	0.65
Environmental						
Type A (good scans &all days)	4.1	4.4	4.5	4.4	4	3.2
(good days only)*	***0.80***	***0.83***	***0.87***	***1.02***	***0.64***	***1.31***
Temporal overlap	0.3	0.3	0.3	0.3	0.3	0.3
Self-shading (uncorrected)	1	1	1.2	1.75	2.5	12
(corrected)*	***0.200***	***0.200***	***0.240***	***0.350***	***0.500***	***2.400***
In-water bio-fouling	1	1	1	1	1	1
Combined Standard Uncertainty	4.7	4.8	5.1	5.1	5.2	12.5
Combined Standard Uncertainty*	***2.4***	***2.1***	***2.4***	***2.3***	***2.4***	***3.3***

environmental conditions. Radiometric calibrations are performed before and after each deployment. Summarized pre-deployment to post-deployment radiometric response ratio's for the MOBY time series are shown in **Fig. 5**. For most, but not all, deployments, the post-deployment responsivity is less than the pre-deployment responsivity. To obtain an uncertainty associated with system response changes representative of the time series, we take the mean absolute difference between pre-and post-deployment calibrations and the standard deviation of those differences over the full time series and assume a rectangular probability distribution over the range from no difference to the mean absolute

difference plus one standard deviation. Figure 6 shows the time series results for the Top, Middle and Bottom arms. For the 412 nm channel, the upper limit is 5.5 %, for the 442 nm channel, 4.5 %, etc. Following the ISO Guide to Uncertainty in Measurement [14], the uncertainty associated with a rectangular probability distribution between two limits is the magnitude of the difference between the limits divided by the square root of 12. This is the system response uncertainty listed in Table 1.

The in-water internal calibration uncertainty represents the standard deviation of internal reference source (LED and incandescent lamp) measurements taken at the same time as the in-water up-welling radiance measurements over one deployment. The uncertainty listed in the table represents an upper limit for this component, and includes the variability in the sources themselves. The uncertainty in the wavelength stability represents the radiometric uncertainty associated with a 1-pixel uncertainty, the maximum deviation observed, in the measurement of atmospheric Fraunhofer lines observed in the E_s measurements over a deployment.

There are two lines in the uncertainty budget for both the Type A environmental uncertainty and the uncertainty associated with self-shading. The two uncertainty components are propagated through to the combined standard uncertainty. The top combined standard uncertainty line used the first of the two uncertainty components associated with Type A environmental uncertainty and the self-shading component, respectively. The bottom combined standard uncertainty used the second line of those two components.

For the Type A environmental uncertainty, the two components reflect the Type A uncertainty for quality-assessed data labeled as good scans and quality-assessed data labeled good scans and good days only. Histograms of the two uncertainty distributions for deployment 31 are shown in Fig. 7. Good scan data have uncertainties as large as 50 % due to rapidly changing environmental conditions, such as can be observed during cloudy days. Data labeled good scans and good data comprise approximately 50 % of the full data set. The uncertainty distribution for this subset of data, shown as solid lines in Fig. 7, is greatly reduced, with uncertainties less than 3 % comprising all but one outlier in the entire data set. The outlier uncertainty in the distribution is 9.5 %. Note that satellite sensor vicarious calibration uses a subset of the good data to reflect only optimal conditions.

Instrument self-shading is included in the uncertainty budget as both uncorrected and corrected components. James Mueller recently completed an extensive modeling study of the magnitude of self-shading for the MOBY system under a variety of solar zenith angles, buoy orientation, and chlorophyll concentrations [15]. Results reproduced from that report, shown in Fig. 8, show the calculated shadowing correction factor for MOBY for a solar zenith angle of 30^o and azimuth angle of 180^o (*i.e.*directly away from the buoy, as seen at the sensor aperture), a backscattering fraction of the particle scattering phase function b_{bp}=0.10, and chlorophyll concentrations of 0.10 mg/m^3 and 0.20 mg/m^3, respectively. The uncorrected self-shadowing correction uncertainty comes from Fig. 8. Field experiments are on-going to empirically validate the calculated results. We expect the correction to reduce the

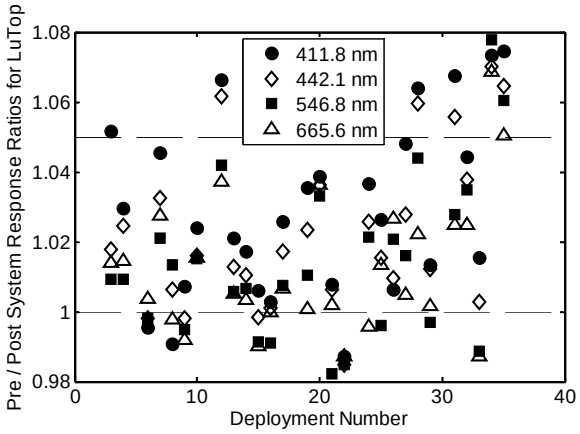

Fig. 5. Pre-deployment to post-deployment system response ratio.

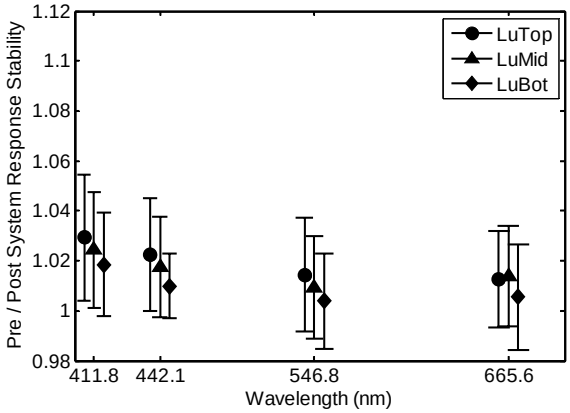

Fig. 6. Mean absolute system response ratio. Error bars correspond to the standard deviation of the mean ratio.

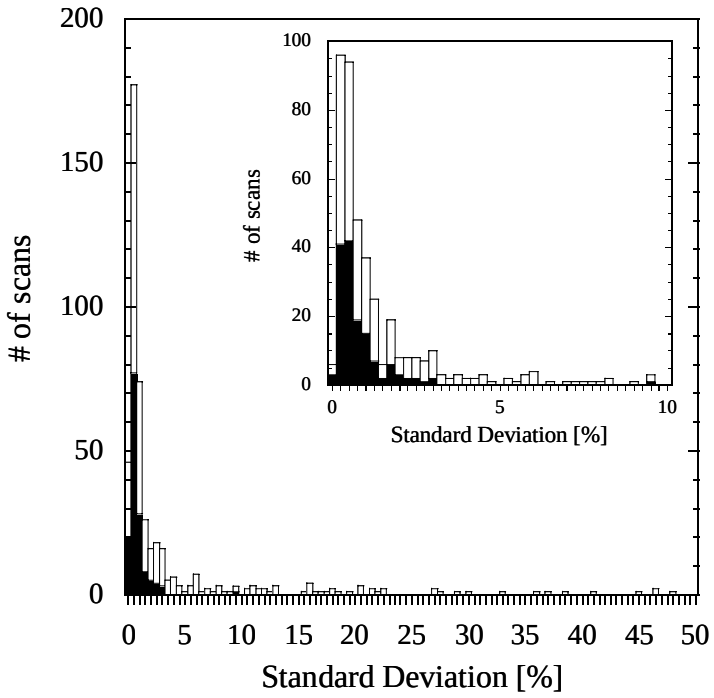

Fig. 7. Clear rectangles, standard deviation of up-welling radiance measured by the top MOBY arm for deployment 31 for all data marked as good scans. Solid rectangles, standard deviation of the up-welling radiance for data marked as good scans and good days; 0.5 % bins. Insert: expanded view with 0.25 % bins.

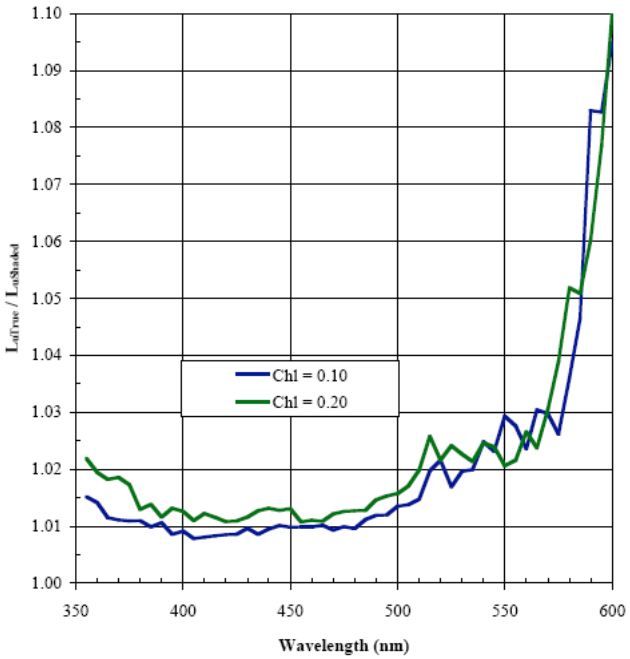

Fig. 8. Spectral distribution of MOBY self-shading factors for backscattering coefficient of 0.01, a solar zenith angle of 30 ^{o} and azimuth angle of 180 ^{o}, and phytoplankton chlorophyll-*a* concentrations of 0.10 mg/m^{3}and 0.20 mg/m^{3}.

uncertainty a factor of 5 (approximately) over the uncorrected uncertainty. This is reflected in the predicted residual uncertainty in the corrected self-shading term. The shadowing contribution depends on the solar zenith and azimuth angles. Uncorrected, we expect seasonal variations for the red channels, e.g. MODIS channel 13, to be of a large enough magnitude to be observed by the satellite sensor.

Summarizing the uncertainty in up-welling radiance, if we take the full data set marked 'good scans' and don't include a shadowing correction, the uncertainty is approximately 5 % for MODIS channels 8 through 12, increasing to 12.5 % for channel 13 due to a large shadowing correction. If only data from good scans labeled good days after quality control checks are applied and a shadowing correction is applied to the data set, we expect a combined standard uncertainty of less than 3 % for MODIS channels 8 through 12, increasing slightly, to 3.3 %, for channel 13.

5. VALIDATION ACTIVITIES

To maintain the spectral radiance and irradiance scales of the sources between calibrations, MOBY sources are monitored routinely with a pair of NIST-developed and calibrated single-channel, temperature-stabilized filter radiometers called Standard Lamp Monitors (SLMs) [7]. The short-wavelength SLM has a band center wavelength of 411.8 nm and a bandwidth of 10.7 nm. The long-wavelength SLM has a center wavelength of 872.2 nm and a bandwidth of 12.3 nm. The SLMs have fore-optics with a well-defined field-of-view of 5^o for radiance measurements. For irradiance measurements, the fore-optics are replaced with a transmissive diffuser. The uncertainty of their radiance and irradiance measurements is estimated to be 1.5 % (k=1). In addition, annual on-site calibration validation checks of the sources are performed by NIST personnel using NASA's SeaWiFS Transfer Radiometer (SXR) (1994 and 1996), Visible Transfer Radiometer (VXR) (8 times since 1999) [16] and a portable radiance standard source [17]. The uncertainties in the transfer radiometers and the radiance source standard is estimated to be 2 % (k=1).

Typically the uncertainties in a radiometric measurement at a particular facility are validated through comparisons with other independent laboratories and institutions. For example, at the National Metrology Level, key measurement comparisons organized by the International Bureau of Weights and Measures (BIPM) under the Treaty of the Meter establish the degree of equivalence between national laboratories [18]. Community validation of the MOBY radiometric scales stems from the second SIMBIOS Radiometric Intercomparison, SIMRIC-2 [19], where the observed differences between expected and measured radiances of MOBY sources were within the combined uncertainties of the source and the SIMRIC-2 transfer radiometer. More recently, MOBY participated in the Spectral Ocean Radiance Transfer Investigation and Experiment (SORTIE), where radiometers from the Center for Hydro-Optics and Remote Sensing (San Diego, CA), WET Labs (Philomath, OR), Satlantic (Halifax, Nova Scotia), and Dalhousie University (Halifax, Nova Scotia) were intercompared with MOBY transfer radiometers and sources in the laboratory. The instruments subsequently measured the upwelling radiance concurrently with MOBY at the MOBY site. Results from this comparison campaign are still being finalized.

6. DISCUSSION

Franz *et al*. recently discussed the vicarious calibration of SeaWiFS ocean color bands using MOBY [3]. MOBY retrievals from September 1997 through March 2006 were analyzed. Franz *et al*. found no time dependence to the vicarious calibration, corroborating the maintenance of the calibration of MOBY over that time period. No dependence was observed as a function of solar zenith angle, for angles ranging from 7.5^o to 55^o; nor any dependence on sensor view angle, for sensor view angles ranging from 22.5^o to 55^o.

The lack of dependence of the vicarious calibration gain coefficient with solar zenith angle is not consistent with Mueller's recent calculations on the self-shading effect, though data were only shown for SeaWiFS 443 nm and 555 nm channels, whereas instrument self-shading is expected to be significant primarily for the SeaWiFS 670 nm channel. The standard deviation of the time series data ranged from 0.9 % for the 412 nm channel to 0.7 % for the 670 nm channel. These uncertainties, propagated to the ocean's surface, would correspond to approximately a 9 % uncertainty in water-leaving radiance for the 412 nm (and other visible) ocean color channels. This is not reflected in the uncertainty budget, where the Type A random uncertainty in water-leaving radiance (Table 2: good scans and good days) is approximately 1 % and the total combined standard uncertainty is approximately 3 %. The water-leaving radiance as determined at the MOBY site is only one component of the vicarious calibration uncertainty budget. Other components include the site homogeneity, atmospheric correction, corrections for the satellite sensor view geometry, and intrinsic satellite sensor signal-to-noise.

Table 2. Uncertainty in L_w

Uncertainty Component [%]	8	9	10	11	12	13
	411.8 nm	442.1 nm	486.9 nm	529.7 nm	546.8 nm	665.6 nm
Good scans and good days	1.00	1.05	1.10	1.48	1.59	2.34

Clearly, attention must be paid to the total uncertainty budget to understand the origin of the dominant sources of uncertainty in the vicarious calibration of SeaWiFS and other ocean color satellite sensors.

The MOBY system is a decade old and in need of refurbishment or replacement. In designing a new buoy system, several improvements are under consideration, using the uncertainty budget for guidance. The two dominant environmental uncertainty components are the Type A random component from environmental fluctuations and self-shading by the buoy itself on the up-welling radiance measurements. Reducing the size of the buoy arms and the radiance heads and eliminated the anti-fouling tubes currently located at the radiance heads will minimize effects of self-shading on the up-welling radiance. Increasing the responsivity of the system, enabling more statistical averaging, and taking measurements from all input ports simultaneously instead of sequentially should reduce the environmental uncertainty component. Recently, a series of in-water proof-of-principle demonstration tests were done in the waters off of Oahu, Hawaii using a small research vessel and a mock-up miniature buoy and acquisition system capable of the simultaneous acquisition of 5 channels of data [20]. With this system, 100 scans could be taken from independent sensor channels in the same time as 5 scans from each channel with the current MOBY system.

The standard deviation of the mean of the water-leaving radiance is shown in Fig. 9 as a function of the number of scans averaged. These measurements were repeated several times with similar results. Averaging 50 scans, the standard deviation of the mean water-leaving radiance is on the order of 0.2 % for the 412 nm, the 442 nm and the 547 nm channels, and approximately 0.5 % for the 666 nm channel. At this level, the Type A uncertainty will not significantly contribute to the combined standard uncertainty in the measurement. The up-welling radiance measured by the individual sensors is highly correlated. We can evaluate the effect of correlations on the water-leaving radiance by comparing the Type A uncertainty in water-leaving radiance using synchronous data and non-synchronous up-welling radiance data from the arms at different depths to calculate the water-leaving radiance. Figure 10 shows the results of that analysis, with the non-synchronous data from individual arms separated by approximately 1 min. Synchronous acquisition of the up-welling radiance reduces the uncertainty in the measured water-leaving radiance approximately 20 % for the blue channels, 35 % for the green channels, and 60 % for the red channels.

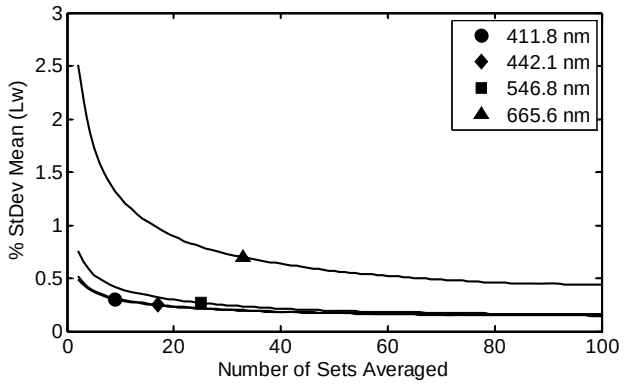

Fig. 9. Percent standard deviation of the mean water-leaving radiance as a function of the number of sets averaged.

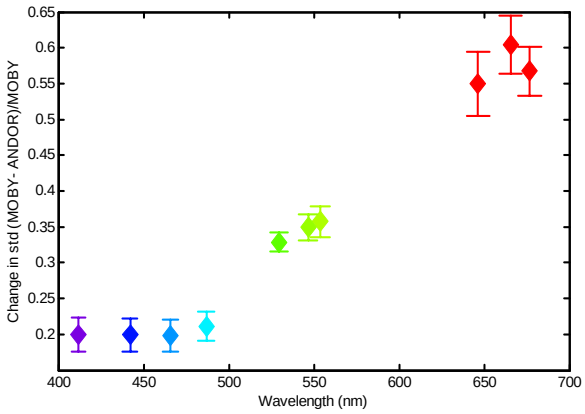

Fig. 10. Ratio of the standard deviation in water-leaving radiance for correlated to uncorrelated up-welling radiance measurements.

7. CONCLUSIONS

Work is on-going to empirically validate the modeled self-shadowing results of Mueller and to establish the final uncertainty budget in the MOBY water-leaving radiance decadal time series. Once the MOBY water-leaving radiance uncertainty budget is established, a rigorous uncertainty analysis of the vicarious calibration of a satellite sensor, e.g. SeaWiFS, can begin. An understanding of the dominant uncertainty components in the satellite sensor vicarious calibration is critical to give guidance for research activities working toward potential reductions in the uncertainty in the vicarious calibration of ocean color satellite sensors.

Establishing measurement traceability to the SI is critical for the proper interpretation of merged, multi-national, multi-sensor ocean color data sets, in particular in the GEOSS-era. The MOBY project, through NOAA-NASA-NIST collaborative efforts, established a robust uncertainty budget and SI-traceable water-leaving radiance measurements at its mooring site in the Hawaiian waters off of Lanai. Through consistent adherence to rigorous calibration protocols and extensive quality control checks on the data set, a combined standard uncertainty in the up-welling radiance measured by the top MOBY arm of less than 3 % for MODIS ocean color channels 8 through 12 and slightly higher than 3 % for channel 13 may be achievable, once the shadowing corrections are applied to the data set. The MOBY experience suggests that, if instruments are properly maintained and calibrated and the data are rigorously quality-checked, long-term radiometric measurements with uncertainties at the 3 % level are possible in marine environments. Extensive analysis of decadal measurements of the Hawaiian waters in the region of MOBY by SeaWiFS recently published by Franz *et al*. [3] shows no temporal trends to the data, nor any seasonal or geometric biases. The consistency in the MOBY-SeaWiFS time series match-up database, in addition to providing a vicarious calibration for SeaWiFS, validates the precision of the historical MOBY data record.

8. ACKNOWLEDGEMENTS

Dennis Clark was supported by Space Dynamics Laboratory, Logan, Utah under a Joint NIST/Utah State University Program in Optical Sensor Calibration. This work was funded in part by NASA under order number NNG04HK33I to NOAA.

REFERENCES

1 Yoder, J., University of Rhode Island, Narragansett, RI 02882.
2 Gordon, H.R., In-orbit calibration strategy for ocean color sensors. Remote Sensing of Environment, 1998. **63**: p. 265-278.
3 Franz, B.A., et al., Sensor-independent approach to the vicarious calibration of satellite ocean color radiometry. Appl. Opt., 2007. **46**: p. 5068-5082.
4 Clark, D.K., et al., MOBY, a radiometric buoy for performance monitoring and vicarious calibration of satellite ocean color sensors: measurement and data analysis protocols, in Ocean Optics Protocols for Satellite Ocean Color Sensor Validation, Revision 4, Volume 6, J.L. Mueller, G.S. Fargion, and C.R. McClain, Editors. 2003, NASA Goddard Space Flight Center: Greenbelt, MD. p. 3-34.
5 IOCCG (2007). Ocean-Colour Data Merging, in Reports of the International Ocean-Colour Coordinating Group, No. 6, IOCCG, W. Gregg, Editor. 2007: Dartmouth, Canada.
6 International Vocabulary of Basic and General Terms in Metrology (VIM), BIPM, IEC, IFCC, ISO, IUPAC, IUPAP, OIML, 2nd ed., 1993, definition 6.10.
7 Clark, D.K., et al., An overview of the radiometric calibration of MOBY. Proc. SPIE, 2002. **4483**: p. 64-76.
8 Clark, D.K., et al., Validation of atmospheric correction over the oceans. J. Geophys. Res., 1997. **102**: p. 17,209-17,217.
9 Austin, R.W., The remote sensing of spectral radiance from below the ocean surface, in Optical Aspects of Oceanography, N.G. Jerlov and E.S. Nelson, Editors. 1974, Academic Press, New York. p. pp. 317-344.
10 Voss, K.J. and A. Morel, Bidirectional reflectance function for oceanic waters with varying chlorophyll concentrations: Measurements versus predictions. Limnol. Oceanogr., 2005. **50**: p. 698-705.
11 Voss, K.J., A. Morel, and D. Antoine, Detailed validation of the bidirectional effect in various Case 1 waters for application to Ocean Color imagery. submitted to Biogeosciences, 2007.

12 Brown, S.W., et al., Stray-light correction of the Marine Optical Buoy, in Ocean Optics Protocols for Satellite Ocean Color Sensor Validation, Revision 4, Volume 6, J.L. Mueller, G.S. Fargion, and C.R. McClain, Editors. 2003, NASA's Goddard Space Flight Center: Greenbelt, MD. p. 87-124.
13 Zong, Y., et al., Simple spectral stray light correction method for array spectroradiometers. Appl. Opt., 2006. **45**: p. 1111-1119.
14 International Standardization Organization, Guide to the expression of uncertainty in measurement, GUM. 1993: Geneva, Switzerland.
15 Mueller, J., Self-shading corrections for MOBY upwelling radiance measurements, in Final Technical Report to NESDIS, NOAA Grant NA04NES44000007. 2007. p. 33.
16 Johnson, B.C., et al., System-level calibration of a transfer radiometer used to validate EOS radiance scales. International Journal of Remote Sensing, 2003. **24**: p. 339-356.
17 Brown, S.W. and B.C. Johnson, A portable integrating sphere source for radiometric calibrations from the visible to the shortwave infrared. The Earth Observer, 1999. **11**: p. 14-19.
18 Treaty of the Meter, http://www.bipm.org/en/convention/.
19 Meister, G., The second SIMBIOS radiometric intercomparison (SIMRIC-2), March-November 2002. NASA/TM-2002-210006 Vol. 2. 2003, Greenbelt, MD: NASA Goddard Space Flight Center.
20 Yarbrough, M., et al., Simultaneous measurement of up-welling spectral radiance using a fiber-coupled CCD spectrograph. Proc. SPIE, 2007. **6680**: p. 6680-18.